# 12

# Tunnels in weak rock

## 12.1 Introduction

Tunnelling in weak rock presents some special challenges to the geotechnical engineer since misjudgements in the design of support systems can lead to very costly failures. In order to understand the issues involved in the process of designing support for this type of tunnel it is necessary to examine some very basic concepts of how a rock mass surrounding a tunnel deforms and how the support systems acts to control this deformation. Once these basic concepts have been explored, examples of practical support designs for different conditions will be considered.

## 12.2 Deformation around an advancing tunnel

Figure 12.1 shows the results of a three-dimensional finite element analysis of the deformation of the rock mass surrounding a circular tunnel advancing through a weak rock mass subjected to equal stresses in all directions. The plot shows displacement vectors in the rock mass as well as the shape of the deformed tunnel profile. Figure 12.2 gives a graphical summary or the most important features of this analysis.

Deformation of the rock mass starts about one half a tunnel diameter ahead of the advancing face and reaches its maximum value about one and one half diameters behind the face. At the face position about one third of the total radial closure of the tunnel has already occurred and the tunnel face deforms inwards as illustrated in Figures 12.1 and 12.2. Whether or not these deformations induce stability problems in the tunnel depends upon the ratio of rock mass strength to the in situ stress level, as will be demonstrated in the following pages.

Note that it is assumed that deformation process described occurs immediately upon excavation of the face. This is a reasonable approximation for most tunnels in rock. The effects of time dependent deformations upon the performance of the tunnel and the design of the support system will be not be discussed in this chapter.

## 12.3 Tunnel deformation analysis

In order to explore the concepts of rock support interaction in a form which can readily be understood, a very simple analytical model will be utilised. This model involves a circular tunnel subjected to a hydrostatic stress field in which the horizontal and vertical stresses are equal.

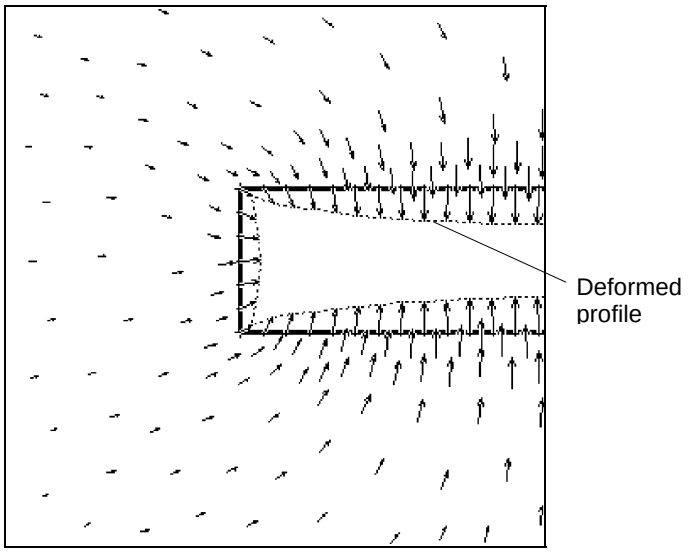


Figure 1: Vertical section through a three-dimensional finite element model of the failure and deformation of the rock mass surrounding the face of an advancing circular tunnel. The plot shows displacement vectors as well as the shape of the deformed tunnel profile.

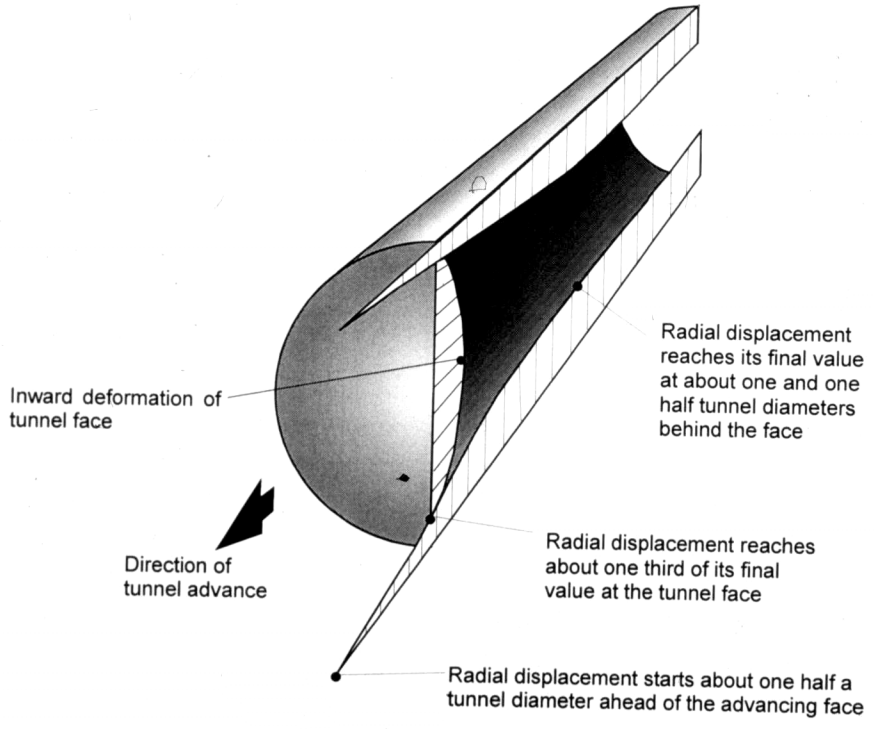


Figure 2: Pattern of deformation in the rock mass surrounding an advancing tunnel.

In this analysis it is assumed that the surrounding rock heavily jointed mass behaves as an elastic-perfectly plastic material in which failure involving slip along intersecting

discontinuities is assumed to occur with zero plastic volume change (Duncan Fama, 1993). Support is modelled as an equivalent internal pressure and, although this is an idealised model, it provides useful insights on how support operates.

### *12.3.1 Definition of failure criterion*

It is assumed that the onset of plastic failure, for different values of the effective confining stress $\sigma_3'$, is defined by the Mohr-Coulomb criterion and expressed as:

$$\sigma_1' = \sigma_{cm} + k\sigma_3' \tag{12.1}$$

The uniaxial compressive strength of the rock mass $\sigma_{cm}$ is defined by:

$$\sigma_{cm} = \frac{2c' \cos\phi'}{(1-\sin\phi')} \tag{12.2}$$

and the slope $k$ of the $\sigma_1'$ versus $\sigma_3'$ line as:

$$k = \frac{(1+\sin\phi')}{(1-\sin\phi')} \tag{12.3}$$

where $\sigma_1'$ is the axial stress at which failure occurs

$\sigma_3'$ is the confining stress

$c'$ is the cohesive strength and

$\phi'$ is the angle of friction of the rock mass

In order to estimate the cohesive strength $c'$ and the friction angle $\phi'$ for an actual rock mass, the Hoek-Brown criterion (Hoek and Brown 1997) can be utilised. Having estimated the parameters for failure criterion, values for $c'$ and $\phi'$ can be calculated as described in Chapter 11.

### *12.3.2 Analysis of tunnel behaviour*

Assume that a circular tunnel of radius $r_o$ is subjected to hydrostatic stresses $p_o$ and a uniform internal support pressure $p_i$ as illustrated in Figure 12.3. Failure of the rock mass surrounding the tunnel occurs when the internal pressure provided by the tunnel lining is less than a critical support pressure $p_{cr}$, which is defined by:

$$p_{cr} = \frac{2p_o - \sigma_{cm}}{1+k} \tag{12.4}$$

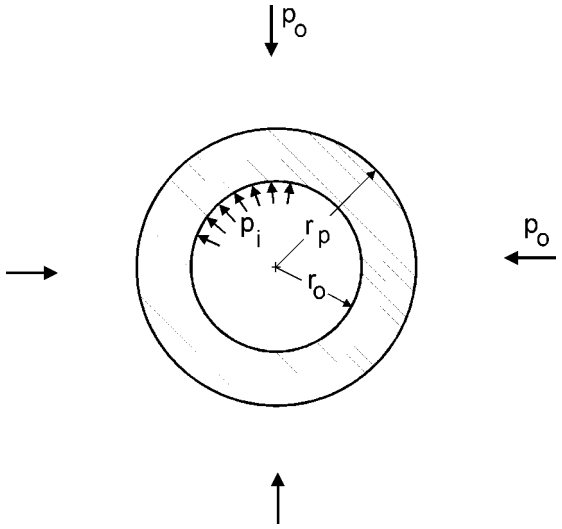


Figure 12.3: Plastic zone surrounding a circular tunnel.

If the internal support pressure $p_i$ is greater than the critical support pressure $p_{cr}$, no failure occurs, the behaviour of the rock mass surrounding the tunnel is elastic and the inward radial elastic displacement of the tunnel wall is given by:

$$u_{ie} = \frac{r_o(1+\nu)}{E_m}(p_o - p_i) \tag{12.5}$$

where $E_m$ is the Young's modulus or deformation modulus and
$\nu$ is the Poisson's ratio.

When the internal support pressure $p_i$ is less than the critical support pressure $p_{cr}$, failure occurs and the radius $r_p$ of the plastic zone around the tunnel is given by:

$$r_p = r_o\left[\frac{2(p_o(k-1)+\sigma_{cm})}{(1+k)((k-1)p_i+\sigma_{cm})}\right]^{\frac{1}{(k-1)}} \tag{12.6}$$

For plastic failure, the total inward radial displacement of the walls of the tunnel is:

$$u_{ip} = \frac{r_o(1+\nu)}{E}\left[2(1-\nu)(p_o - p_{cr})\left(\frac{r_p}{r_o}\right)^2 - (1-2\nu)(p_o - p_i)\right] \tag{12.7}$$

A spreadsheet for the determination of the strength and deformation characteristics of the rock mass and the behaviour of the rock mass surrounding the tunnel is given in Figure 12.4.

**Input:**

| | | | | | | | | |
|---|---|---|---|---|---|---|---|---|
| sigci = | 10 | MPa | mi = | 10 | | GSI = | 25 | |
| mu = | 0.30 | | ro = | 3.0 | m | po = | 2.0 | Mpa |
| pi = | 0.0 | MPa | pi/po = | 0.00 | | | | |

**Output:**

| | | | | | | | | |
|---|---|---|---|---|---|---|---|---|
| mb = | 0.69 | | s = | 0.0000 | | a = | 0.525 | |
| k = | 2.44 | | phi = | 24.72 | degrees | coh = | 0.22 | MPa |
| sigcm = | 0.69 | MPa | E = | 749.9 | MPa | pcr = | 0.96 | MPa |
| rp = | 6.43 | m | ui = | 0.0306 | m | ui= | 30.5957 | mm |

| | | | |
|---|---|---|---|
| sigcm/po | 0.3468 | rp/ro = 2.14 | ui/ro = 0.0102 |

**Calculation:**

| | | | | | | | | | Sums |
|---|---|---|---|---|---|---|---|---|---|
| sig3 | 1E-10 | 0.36 | 0.71 | 1.1 | 1.43 | 1.79 | 2.14 | 2.50 | 10.00 |
| sig1 | 0.00 | 1.78 | 2.77 | 3.61 | 4.38 | 5.11 | 5.80 | 6.46 | 29.92 |
| sig3sig1 | 0.00 | 0.64 | 1.98 | 3.87 | 6.26 | 9.12 | 12.43 | 16.16 | 50 |
| sig3sq | 0.00 | 0.13 | 0.51 | 1.15 | 2.04 | 3.19 | 4.59 | 6.25 | 18 |

**Cell formulae:**

mb = mi*EXP((GSI-100)/28)
s = IF(GSI>25,EXP((GSI-100)/9),0)
a = IF(GSI>25,0.5,0.65-GSI/200)
sig3 = Start at 1E-10 (to avoid zero errors) and increment in 7 steps of sigci/28 to 0.25*sigci
sig1 = sig3+sigci*(((mb*sig3)/sigci)+s)^a
k = (sumsig3sig1 - (sumsig3*sumsig1)/8)/(sumsig3sq-(sumsig3^2)/8)
phi = ASIN((k-1)/(k+1))*180/PI()
coh = (sigcm*(1-SIN(phi*PI()/180)))/(2*COS(phi*PI()/180))
sigcm = sumsig1/8 - k*sumsig3/8
E = IF(sigci>100,1000*10^((GSI-10)/40),SQRT(sigci/100)*1000*10^((GSI-10)/40))
pcr = (2*po-sigcm)/(k+1)
rp = IF(pi<pcr,ro*(2*(po*(k-1)+sigcm)/((1+k)*((k-1)*pi+sigcm)))^(1/(k-1)),ro)
ui = IF(rp>ro,ro*((1+mu)/E)*(2*(1-mu)*(po-pcr)*((rp/ro)^2)-(1-2*mu)*(po-pi)),ro*(1+mu)*(po-pi)/E)

Figure 12.4: Spreadsheet for the calculation of rock mass characteristics and the behaviour of the rock mass surrounding a circular tunnel in a hydrostatic stress field.

## 12.4 Dimensionless plots of tunnel deformation

A useful means of studying general behavioural trends is to create dimensionless plots from the results of parametric studies. Two such dimensionless plots are presented in Figures 12.5 and 12.6. These plots were constructed from the results of a Monte Carlo analysis in which the input parameters for rock mass strength and tunnel deformation were varied at random in 2000 iterations [1]. It is remarkable that, in spite of the very wide range of conditions included in these analyses, the results follow a very similar trend and that it is possible to fit curves which give a very good indication of the average trend.

[1] Using the program @RISK in conjunction with a Microsoft Excel spreadsheet for estimating rock mass strength and tunnel behaviour (equations 4 to 7). Uniform distributions were sampled for the following input parameters, the two figures in brackets define the minimum and maximum values used: Intact rock strength $\sigma_{ci}$ (1,30 MPa), Hoek-Brown constant $m_i$ (5,12), Geological Strength Index GSI (10,35), In situ stress (2, 20 MPa), Tunnel radius (2, 8 m).

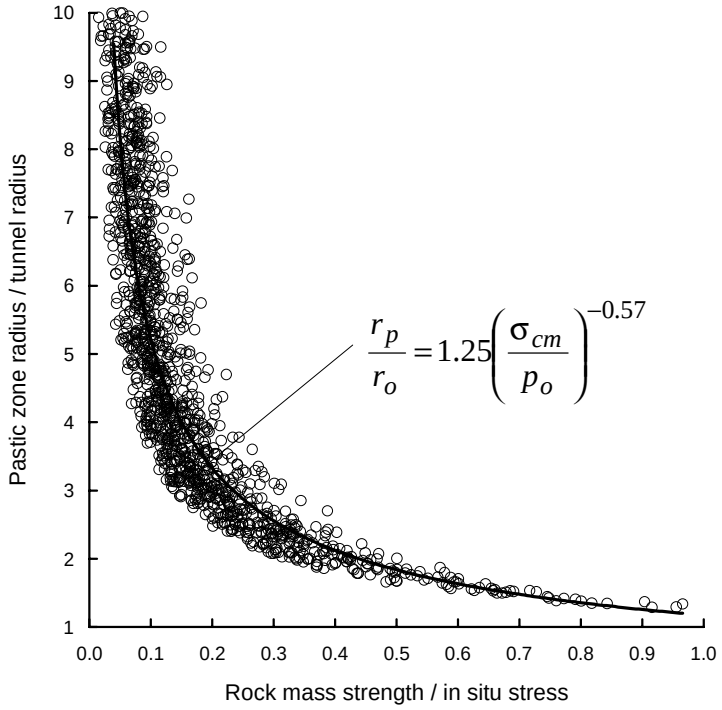


Figure 12.5: Relationship between size of plastic zone and ratio of rock mass strength to in situ stress.

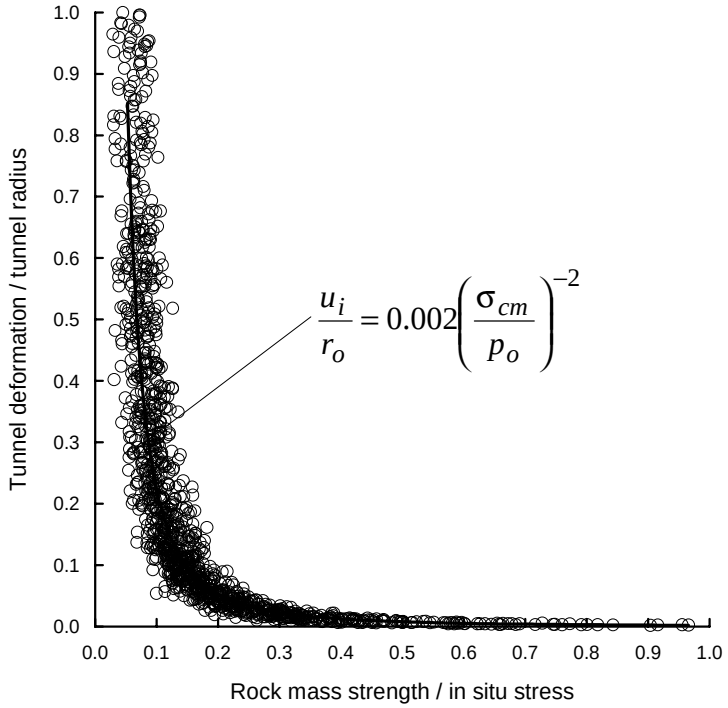


Figure 12.6: Tunnel deformation versus ratio of rock mass strength to in situ stress.

Figure 12.5 gives a plot of the ratio to plastic zone radius to tunnel radius versus the ratio of rock mass strength to in situ stress. This plot shows that the plastic zone size increases very rapidly once the rock mass strength falls below 20% of the rock mass strength. Practical experience suggests that, once this rapid growth stage is reached it becomes very difficult to control the stability of the tunnel.

Figure 12.6 is a plot of the ratio of tunnel deformation to tunnel radius against the ratio of rock mass strength to in situ stress. Once the rock mass strength falls below 20% of the in situ stress level, deformations increase substantially and, unless these deformations are controlled, collapse of the tunnel is likely to occur.

Figures 12.5 and 12.6 are for the condition of zero support pressure ($p_i = 0$). Similar analyses were run for a range of support pressure versus in situ stress ratios ($p_i/p_o$) and a statistical curve fitting process was used to determine the best fit curves for the generated data for each $p_i/p_o$ value. These curves are given in Figures 12.7 and 12.8.

The series of curves shown in Figures 12.7 and 12.8 are defined by the equations:

$$\frac{rp}{ro} = \left(1.25 - 0.625\frac{p_i}{p_o}\right)\sigma_{cm}\left(\frac{p_i}{p_o} - 0.57\right) \tag{12.8}$$

$$\frac{ui}{ro} = \left(0.002 - 0.0025\frac{p_i}{p_o}\right)\frac{\sigma_{cm}}{p_o}\left(2.4\frac{p_i}{p_o} - 2\right) \tag{12.9}$$

where $rp$ = Plastic zone radius
$u_I$ = Tunnel sidewall deformation
$r_o$ = Original tunnel radius in metres
$p_I$ = Internal support pressure
$p_o$ = In situ stress = depth below surface × unit weight of rock mass
$\sigma_{cm}$= Rock mass strength = $2c' \cos\phi' /(1-\sin\phi')$

An alternative plot of the data used to construct Figure 12.8 is given in Figure 12.9. For readers who have studied rock support interaction analyses this plot will be familiar and it gives a good indication of the influence of support pressures on tunnel deformation.

## 12.5 Estimates of support capacity

Hoek and Brown (1980a) and Brady and Brown (1985) have published equations which can be used to calculate the capacity of mechanically anchored rockbolts, shotcrete or concrete linings or steel sets for a circular tunnel. No useful purpose would be served by reproducing these equations here but they have been used to estimate the values plotted in Figure 12.10. This plot gives maximum support pressures ($p_{sm}$) and maximum elastic displacements ($u_{sm}$) for different support systems installed in circular tunnels of different diameters. Note that, in all cases, the support is assumed to act over the entire surface of the tunnel walls. In other words, the shotcrete and concrete linings are closed rings; the steel sets are complete circles; and the mechanically anchored rockbolts are installed in a regular pattern that completely surrounds the tunnel.

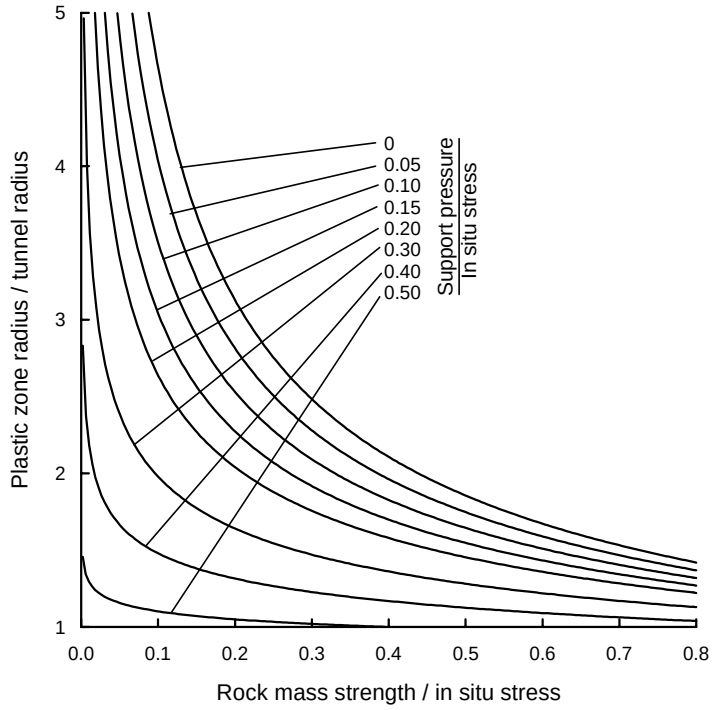


Figure 12.7: Ratio of plastic zone to tunnel radius versus the ratio of rock mass strength to in situ stress for different support pressures.

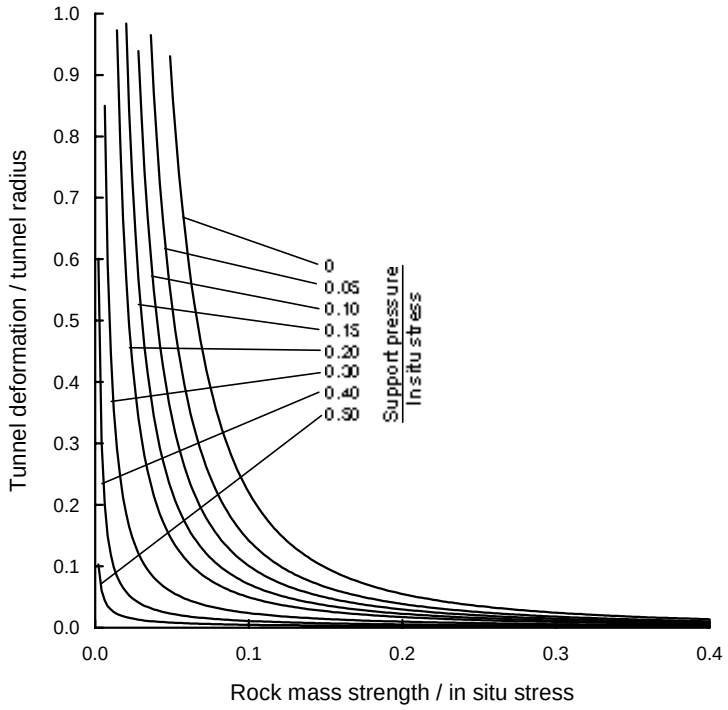


Figure 12.8: Ratio of tunnel deformation to tunnel radius versus the ratio of rock mass strength to in situ stress for different support pressures.

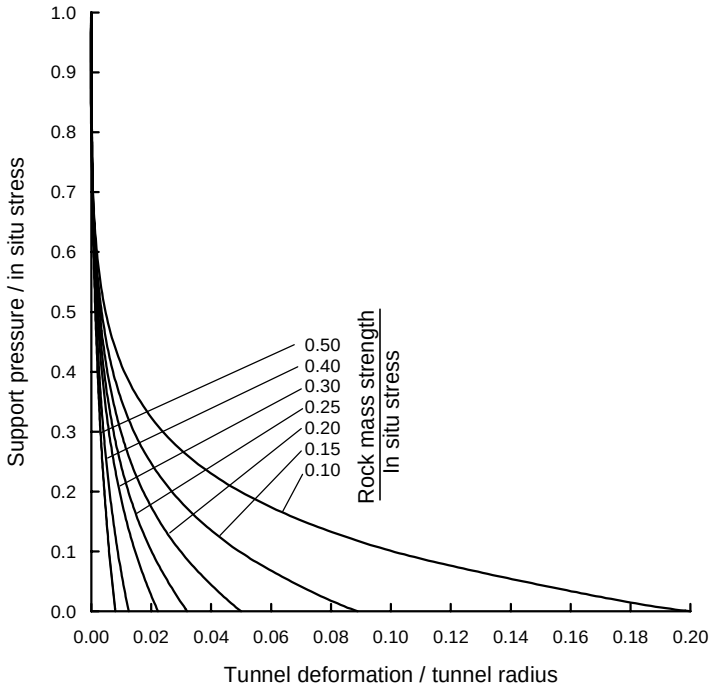


Figure 12.9: Relationship between support pressure and tunnel deformation for different ratios of rock mass strength to in situ stress.

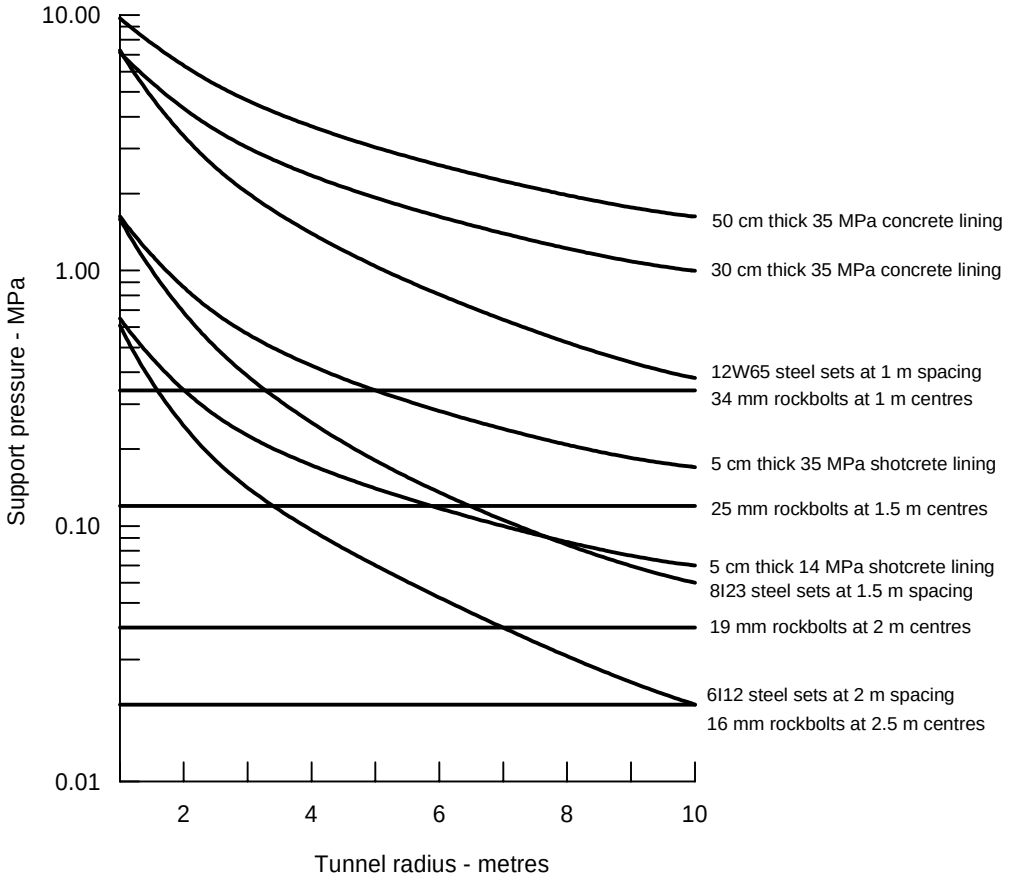


Figure 12.10: Estimates of support capacity for tunnels of different sizes.

Because this model assumes perfect symmetry under hydrostatic loading of circular tunnels, no bending moments are induced in the support. In reality, there will always be some asymmetric loading, particularly for steel sets and shotcrete placed on rough rock surfaces. Hence, induced bending will result in support capacities that are lower than those given in Figure 12.10. Furthermore, the effect of not closing the support ring, as is frequently the case, leads to a drastic reduction in the capacity and stiffness of steel sets and concrete or shotcrete linings.

## 12.6 Practical example

In order to illustrate the application of the concepts presented in this chapter, the following practical example is considered.

A 4 m span drainage tunnel is to be driven in the rock mass behind the slope of an open pit mine. The tunnel is at a depth of approximately 150 m below surface and the general rock is a granodiorite of fair quality. A zone of heavily altered porphyry associated with a fault has to be crossed by the tunnel and the properties of this zone, which has been exposed in the open pit, are known to be very poor. Mine management has requested an initial estimate of the behaviour of the tunnel and of the probable support requirements. The tunnel is to link up with an old mine drainage tunnel that was constructed several decades ago.

### *12.6.1 Estimate of rock mass properties*

Figures 12.6 and 12.7 show that a crude estimate of the behaviour of the tunnel can be made if the ratio of rock mass strength to in situ stress is available. For the purpose of this analysis the in situ stress is estimated from the depth below surface and the unit weight of the rock. For a depth of 150 m and a unit weight of 0.027 MN/m$^3$, the vertical in situ stress is approximately 4 MPa. The fault material is considered incapable of sustaining high differential stress levels and it is assumed that the horizontal and vertical stresses are equal within the fault zone.

It has been found that the ratio of the uniaxial compressive strengths in the field and the laboratory $(\sigma_{cm}/\sigma_{ci})$, calculated by means of the spreadsheet given in Figure 11.7 in Chapter 11 and shown in Figure 12.11, can be estimated from the following equation:

$$\sigma_{cm} = (0.0034m_i^{0.8})\sigma_{ci}\{1.029 + 0.025e^{(-0.1m_i)}\}^{GSI} \qquad (12.10)$$

where *GSI* is the Geological Strength Index and $m_i$ is a material constant as proposed by Hoek and Brown (1997) and discussed in Chapter 11.

In the case of the granodiorite, the laboratory uniaxial compressive strength is approximately 100 MPa. However for the fault material, specimens can easily be broken by hand as shown in Figure 12.12. The laboratory uniaxial compressive strength of this material is estimated at approximately 10 MPa.

Based upon observations in the open pit mine slopes, the granodiorite is estimated to have a GSI value of approximately 55. The fault zone has been assigned GSI = 15. The rock mass descriptions that form the basis of these estimates are illustrated in Figure 12.13.

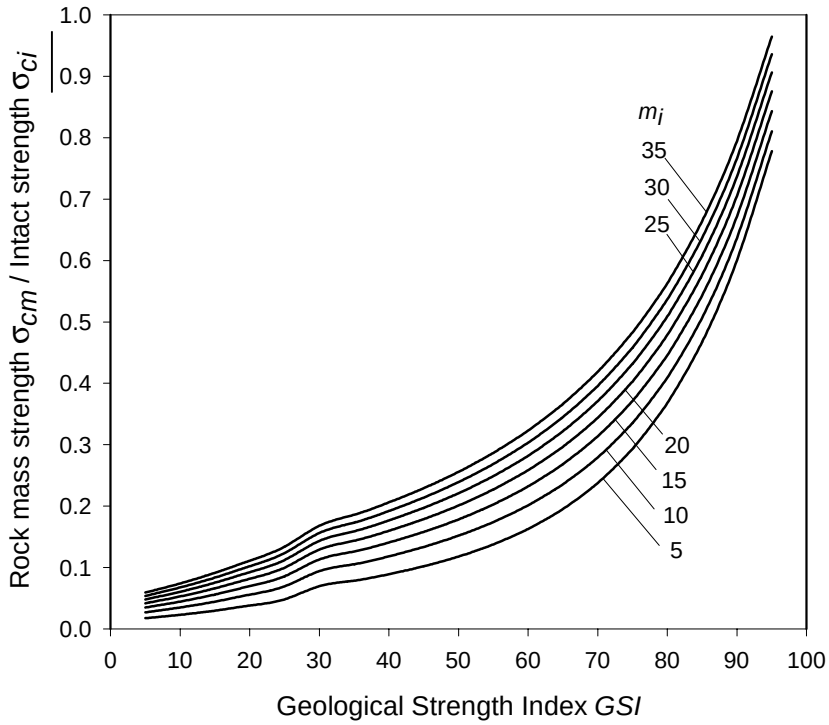


Figure 12.11: Relationship between in situ and laboratory uniaxial compressive strengths and the Geological Strength Index.

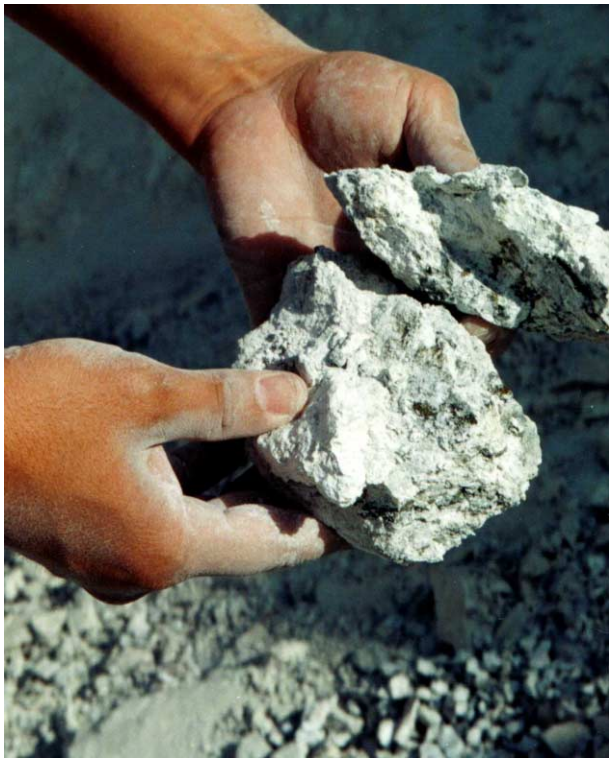

Figure 12.12: Heavily altered porphyry can easily be broken by hand.

Figure 12.13: Table for estimating GSI value (Hoek and Brown 1997) showing ranges of values for granodiorite and fault zone.

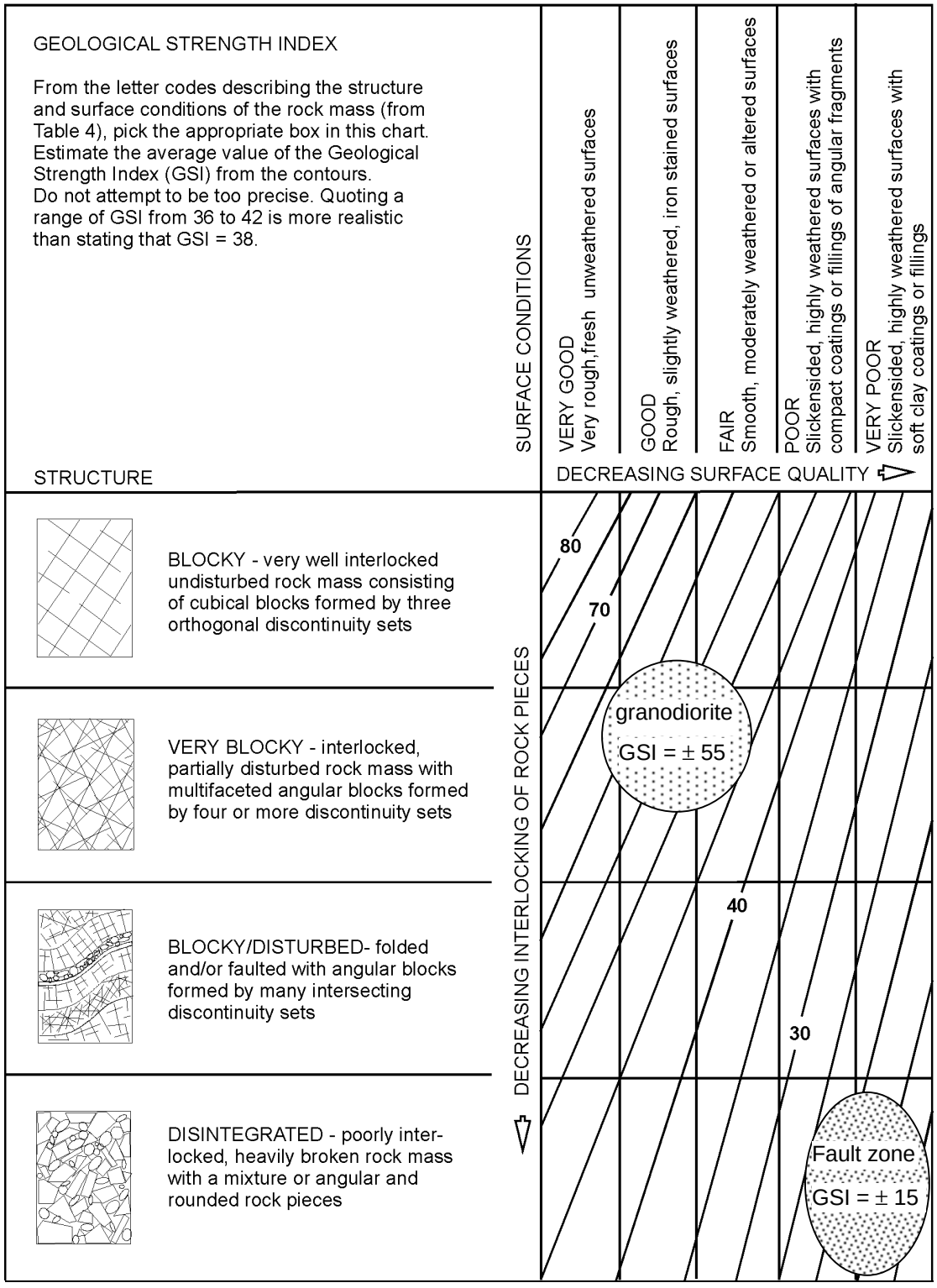

For the granodiorite, substitution of GSI = 55, $m_i$ = 30 and $\sigma_{ci}$ = 100 MPa into equation 12.10 gives an approximate value for the uniaxial compressive strength of the rock mass as 23 MPa. For an in situ stress of 4 MPa, this gives a ratio of rock mass strength to in situ stress in excess of 5. Figures 12.5 and 112.6 show that the size of the plastic zone and also the induced deformations will be negligibly small for is ratio. This conclusion is confirmed by the appearance of the old drainage tunnel that has stood for several decades without any form of support.

Based upon this evaluation, no permanent support should be required for the tunnel in the fair quality granodiorite. Temporary support in the form of spot bolts and shotcrete may be required for safety where the rock mass is heavily jointed.

In the case of the altered porphyry and fault material, substitution of GSI = 15, $m_i$ = 12 and $\sigma_{ci}$ = 10 MPa into equation 12.10 gives a rock mass strength of approximately 0.4. This, in turn, gives a ratio of rock mass strength to in situ stress of 0.1.

From Figure 12.5, the radius of plastic zone for a 2 m radius tunnel in this material is approximately 9.5 m without support. The tunnel deformation in approximately 0.4 m, giving a closure of 0.8 m. These conditions are clearly unacceptable and substantial support is required in order to prevent convergence and possible collapse of this section. Since this is a drainage tunnel, the final size is not a major issue and a significant amount of closure can be tolerated. However, experience suggests that the ratio of tunnel deformation to tunnel radius should be kept below about 0.02 in order to avoid serious instability problems. Figure 12.9 indicates that a ratio of support pressure to in situ stress of approximately 0.35 is required to restrain the deformation to this level for a rock mass with a ratio of rock mass strength to in situ stress of 0.1. This translates into a required support pressure of 1.4 MPa.

Because of the very poor quality of the rock mass and the presence of significant amount of clay, the use of rockbolts or cables is not appropriate because of the difficulty of achieving adequate anchorage. Consequently, support has to be in the form of shotcrete or concrete lining or closely spaced steel sets as suggested by Figure 12.10. Obviously, placement of a full concrete lining during tunnel driving is not practical and hence the remaining choice for support is the use of steel sets.

The problem of using heavy steel sets in a small tunnel is that bending of the sets is difficult. A practical rule of thumb is that an H or I section can only be bent to a radius of about 14 times the depth of the section. This problem is illustrated in Figure 12.14 that shows a heavy H section set being bent. In spite of the presence of temporary stiffeners, there is significant buckling of the inside flange of the set and a lot of additional work is required before the set can be sent underground.

The practical solution adopted in the actual case upon which this example is based was to use sliding joint top hat section sets. These sets, as delivered to site, are shown in Figure 12.15 which illustrates how the sections fit into each other. The assembly of these sets to form a sliding joint is illustrated in Figure 12.16 and the installation of the sets in the tunnel is illustrated in Figure 12.17.

The sets are installed immediately behind the advancing case which, in a rock mass such as that considered here, is usually excavated by hand . The clamps holding the joints are tightened to control the frictional force in the joints which slide progressively as the face is advanced and the rock load is applied to the sets.

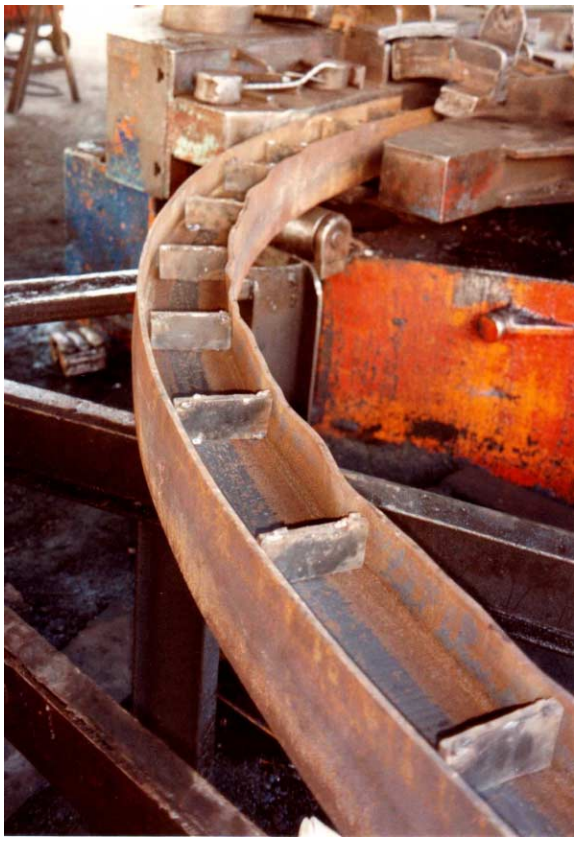

Figure 12.14: Buckling of an H section steel set being bent to a small a radius. Temporary stiffeners have been tack welded into the section to minimise buckling but a considerable amount of work is required to straighten the flanges after these stiffeners have been removed.

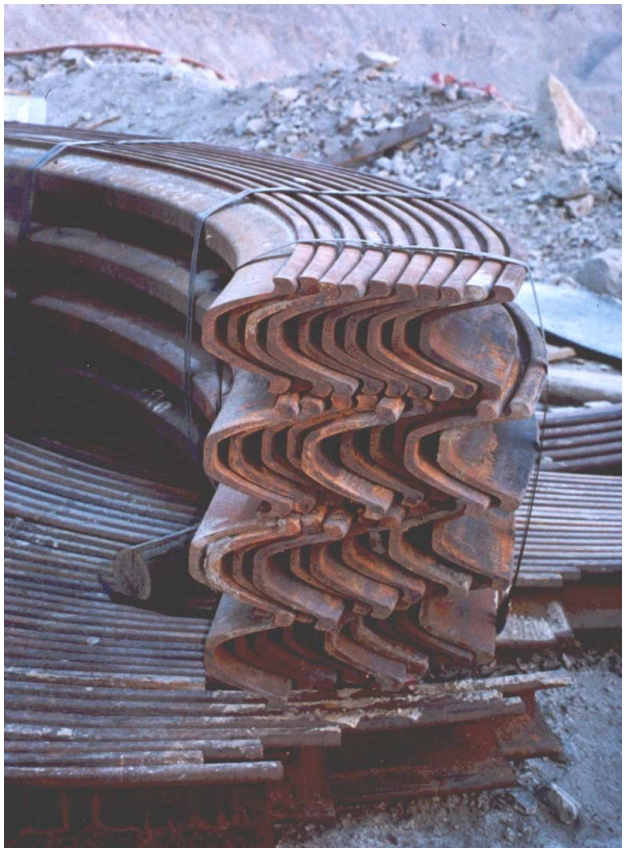

Figure 12.15: Top hat section steel sets delivered to site ready to be transported underground.

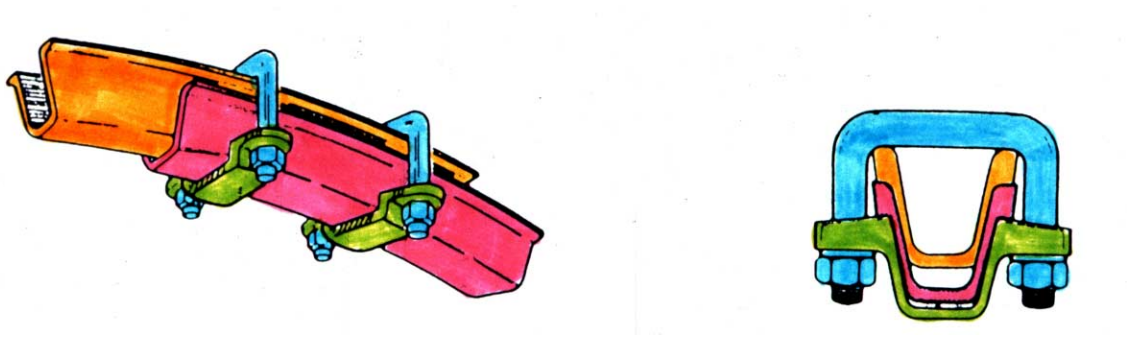

Figure 12.16: Assembly of a friction joint in a top hat section steel set.

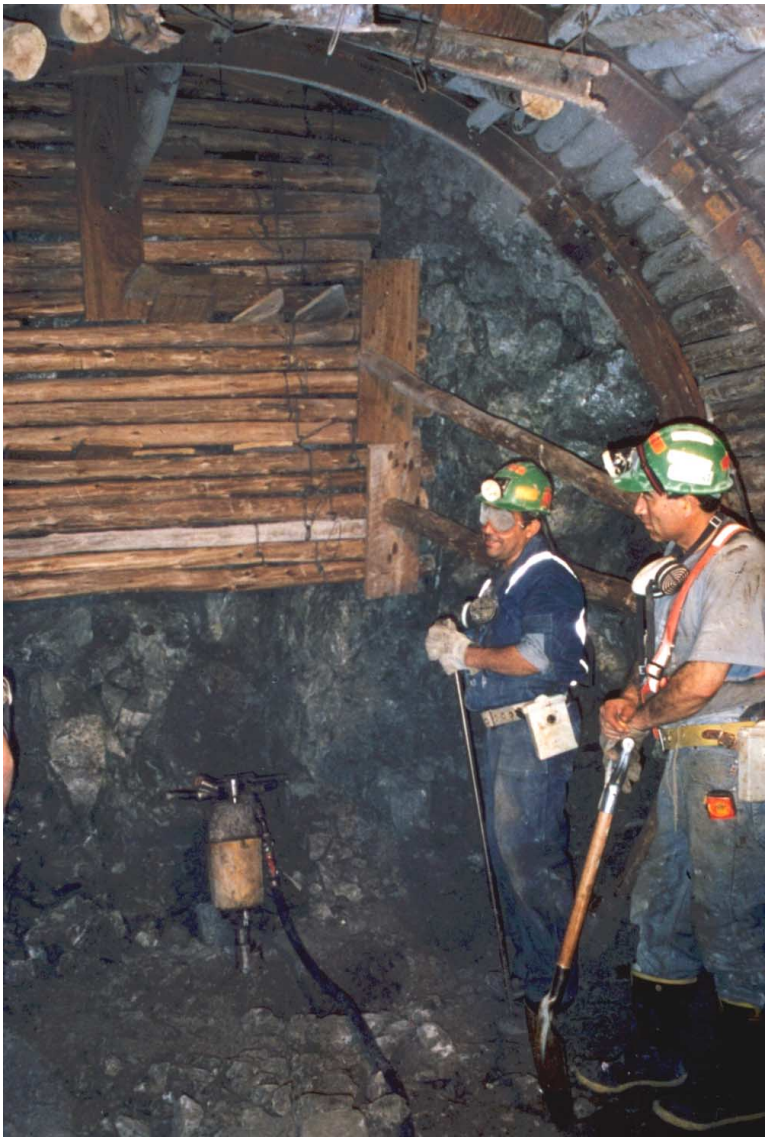

Figure 12.17: Installation of sliding joint top hat section steel sets immediately behind the face of a tunnel being advanced through very poor quality rock.

The use of sliding joints in steel sets allows very much lighter section sets to be used than would be the case for sets with rigid joints. These sets provide immediate protection for the workers behind the face but they permit significant deformation of the tunnel to take place as the face is advanced. In most cases, a positive stop is welded onto the sets so that, after a pre-determined amount of deformation has occurred, the joint locks and the set becomes rigid. A trial and error process has to be used to find the amount of deformation that can be permitted before the set locks. Too little deformation will result in obvious buckling of the set while too much deformation will result in loosening of the surrounding rock mass.

In the case of the tunnel illustrated in Figure 12.17, lagging behind the sets consists of wooden poles of about 100 mm diameter. A variety of materials can be used for lagging but wood, in the form of planks or poles, is still the most common. In addition to the lagging, a timber mat has been propped against the face to improve the stability of the face. This is an important practical precaution since instability of the tunnel face can result in progressive ravelling ahead of the steel sets and, in some cases, collapse of the tunnel.

As an alternative to supporting the face, as illustrated in Figure 12.17, uses spiles to create an umbrella of reinforced rock ahead of the advancing face. Figures 12.18 illustrate the general principles of the technique. In the example illustrated, spiling is being used to advance a 7 m span, 3 m high tunnel top heading through a clay-rich fault zone material in a tunnel in India. The spiles, consisting of 25 mm steel bars, were driven in by means of a heavy sledgehammer.

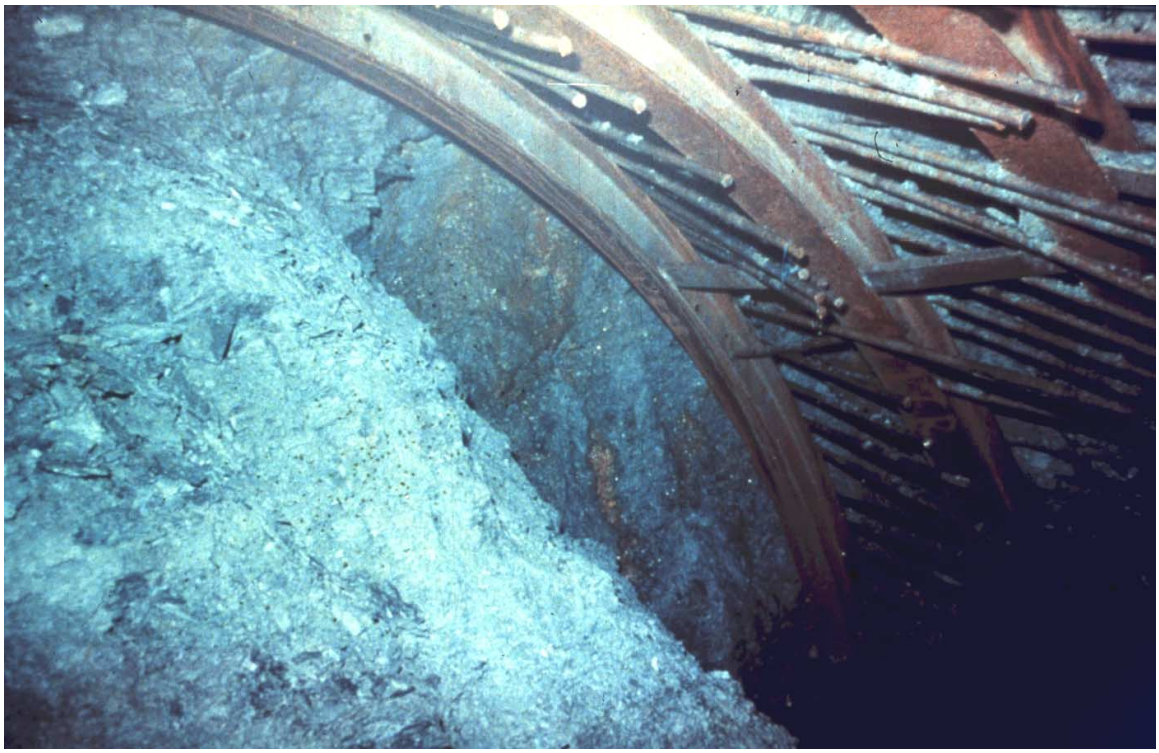

Figure 12.18: Spiling in very poor quality clay-rich fault zone material.

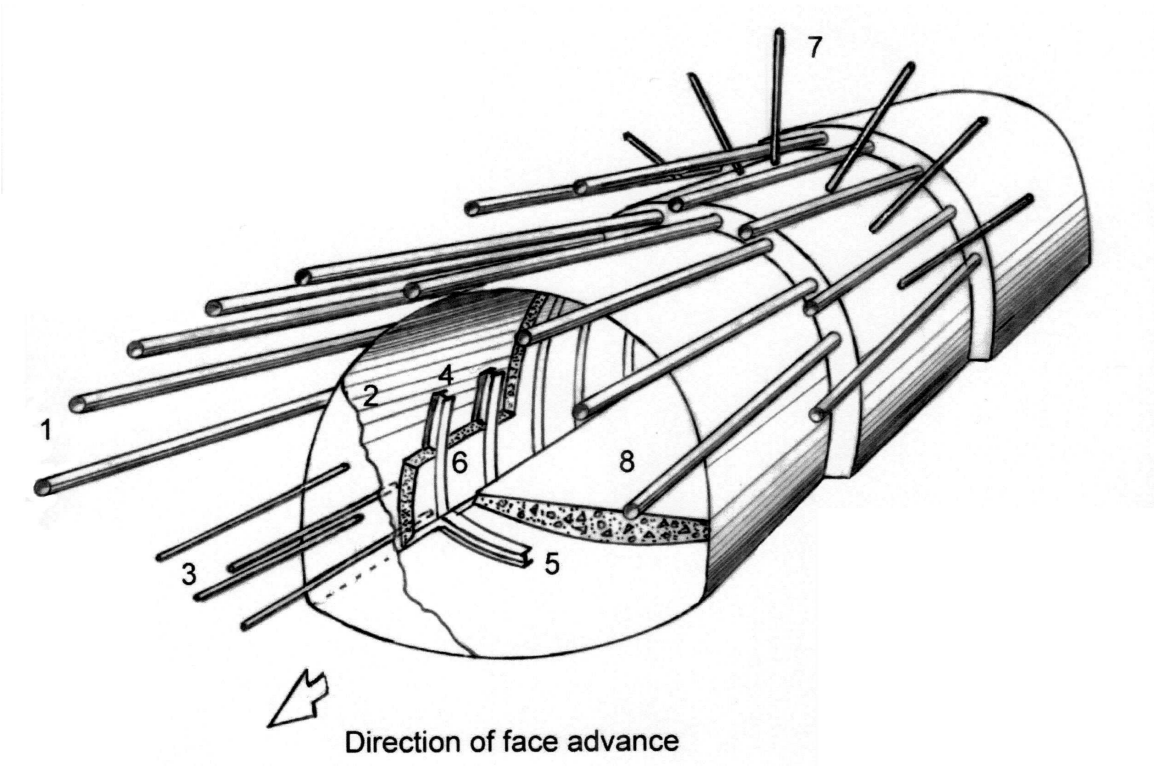


1 Forepoles – typically 75 or 114 mm diameter pipes, 12 m long installed every 8 m to create a 4 m overlap between successive forepole umbrellas.

2 Shotcrete – applied immediately behind the face and to the face, in cases where face stability is a problem. Typically, this initial coat is 25 to 50 mm thick.

3 Grouted fiberglass dowels – Installed midway between forepole umbrella installation steps to reinforce the rock immediately ahead of the face. These dowels are usually 6 to 12 m long and are spaced on a 1 m x 1 m grid.

4 Steel sets – installed as close to the face as possible and designed to support the forepole umbrella and the stresses acting on the tunnel.

5 Invert struts – installed to control floor heave and to provide a footing for the steel sets.

6 Shotcrete – typically steel fiber reinforced shotcrete applied as soon as possible to embed the steel sets to improve their lateral stability and also to create a structural lining.

7 Rockbolts as required. In very poor quality ground it may be necessary to use self-drilling rockbolts in which a disposable bit is used and is grouted into place with the bolt.

8 Invert lining – either shotcrete or concrete can be used, depending upon the end use of the tunnel.

Figure 12.19: Full face 10 m span tunnel excavation through weak rock under the protection of a forepole umbrella. The final concrete lining is not included in this figure.

For larger tunnels in very poor ground, forepoles are usually used to create a protective umbrella ahead of the face. These forepoles consist of 75 to 140 mm diameter steel pipes through which grout is injected. In oder for the forepoles to work effectively the rock mass should behave in a frictional manner so that arches or bridges can form between individual forepoles. The technique is not very effective in fault gouge material containing a siginifcant proportion of clay unless the forepole spacing is very close. The forepoles are in installed by means of a special drilling maching as illustrated in Figure 12.20.

Where the rock mass is suitable for the application of forepoles, consideration can be given to stabilising the face by means of fibreglass dowels grouted into the face as illustrated in Figure 12.19.

Figure 12.20: Installation of 12 m long 75 mm diameter pipe forepoles in an 11 m span tunnel top heading in a fault zone.